A STUDY OF THE RADIANT IGNITION OF A RANGE OF PYROTECHNIC MATERIALS USING A CO_2 LASER

AR-006-315

②

L. de YONG, B. PARK AND F. VALENTA

MRL-TR-90-20

AD-A238 185

DTIC
S ELECTE
JUL 19 1991
C D

MATERIALS RESEARCH LABORATORY

DSTO

A Study of the Radiant Ignition of a Range of Pyrotechnic Materials using a CO_2 Laser

L. de Yong, B. Park[*] and F. Valenta[*]

Abstract

The ignition energy requirements for a range of pyrotechnic compositions of interest in both Australia and the United States have been measured experimentally using a 400 W CO_2 laser operating at 10.6 μm. The effects of several physical and chemical variables were determined on the time to ignition and ignition energy. The materials examined include a gasless delay, igniter compositions, a primer composition and a range of colored smoke compositions. The experimental data serves as a useful probe into ignition mechanisms, and may prove of value in the design of practical ignition systems.

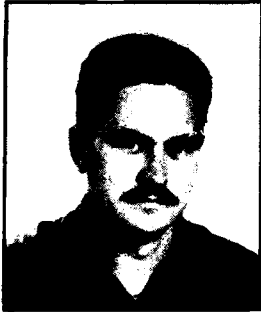[*] Naval Ordnance Station, Indian Head, Maryland, USA

Authors

Leo de Yong graduated BAppSc (Chemistry) in 1977 from University of Melbourne. He worked for ICI Australia (Explosives) and Royal Melbourne Institute of Technology before joining MRL in 1982. His work has focussed on pyrotechnics and their applications.

Brian Park graduated BS Mechanical Engineering from the University of Maryland in 1985 and MSc Engineering from Catholic University of America in 1989. He has worked on cartridge actuated devices and pyrotechnics for rocket motor igniters for 5 years at Naval Ordnance Station, Indian Head, Maryland. He is currently working in the area of hydrodynamic testing at Naval Surface Warfare Centre, White Oak, Maryland, USA.

Frank Valenta graduated BA (Physics) from Catholic University of America, Washington in 1968. He has worked at Naval Ordnance Station, Indian Head, Maryland since then specialising in the areas of pyrotechnics and ordnance devices. He is currently the Special Assistant for Technology at Naval Ordnance Station.

Contents

A Study of the Radiant Ignition of a Range of Pyrotechnic Materials Using a CO_2 Laser

1. Introduction

The ignition sensitivity of a pyrotechnic material to a defined stimulus is a measure of the ability of that material to ignite and undergo sustained combustion when subjected to that stimulus. Most practical methods for evaluating ignition sensitivity suffer from one major problem; energy (and power) absorbed by the composition is imprecisely measured, poorly controlled and assumed to be 100% of the output energy (or power) of the ignition stimulus. The use of a laser, as a controlled ignition source, can overcome this problem to a significant degree.

A laser has several advantages and disadvantages as a practical ignition system and as a research tool. It has the advantage of being able to deliver a precise, programmed and repeatable quantity of radiant energy to the energetic material. Its emission spectrum is monochromatic and essentially independent of environmental parameters (pressure, temperature) which makes the laser ideal for studying ignition behaviour. Ignition systems based on lasers have the advantage of being relatively immune to induced electromagnetic radiation.

However, real ignition systems operate via convective, conductive and radiative energy transfer and are non monochromatic; therefore the laser does not model real ignition systems.

Laser initiation of energetic materials is certainly not new; it has been used widely to initiate propellants [1-3], explosives [4-6] and pyrotechnics [7-9] and to study ignition mechanisms. Use of laser based initiation or fusing systems is seen as a significant advance over current systems particularly its reduced electromagnetic susceptibility. The availability of new, high power laser diodes is also opening up development of small, light weight, self contained laser/fibre optic fusing systems.

The study reported here attempts to expand the data base on the laser initiation of pyrotechnic formulations. New formulations, of interest in both Australia and the United States are examined, in particular the effect of several physical and chemical variables on ignition sensitivity.

2. Radiant Ignition

When a sample is radiatively heated, the incident energy is partitioned between that absorbed, that reflected and that transmitted through the sample. The most important of these for ignition is the absorbed energy. The absorbed energy heats the sample, reactions occur (decomposition, phase changes, etc.) and if the temperature generated is greater than the ignition temperature of the material, ignition will occur at points of thermal concentration ("hot spots"). If the exothermic ignition reaction produces enough energy which, when fed back into the unreacted material, is sufficient to cause ignition in the unreacted material, then the ignition process propagates through the unreacted material leading to sustained combustion. If the exothermic ignition reaction does not produce sufficient energy to sustain combustion, then either the reaction ceases or it may continue only as long as the sample is radiatively heated by the incident laser energy.

Simplistically, the transmitted radiant energy passes directly through the sample and, along with the reflected energy, does not affect the ignition process. Earlier work has also shown that many energetic materials absorb nearly all the incident radiation at 10.6 μm and that transmission and reflection are negligible [10]. The combustion products also absorb some of the incident radiant energy and interact with any reflected radiation adding to the complexity of the radiant ignition process.

3. Ignition Criteria

A common method used to measure ignition sensitivity is the time between commencement of the incident radiation and the first light output (visible and/or IR) from the sample. In this study, we have taken the time to first light to be indicative of the start of the ignition process. After ignition commences rapid visible light output follows, indicating commencement of combustion. The time to first light is accordingly recorded as the time to ignition.

The time to ignition, may be measured in two ways. Firstly, it may be measured as the difference in time between the onset of the laser pulse and the first IR/visible light output. Therefore, it is measured directly from the oscilloscope recording and is designated t_{ig}. Secondly, time to ignition may be measured using the Go/No-Go or Bruceton approach. In this method, the sample is irradiated with a pulse of sufficient length to cause ignition. The pulse length is then reduced and the sample irradiated. This procedure continues until a non-ignition is observed. The pulse length is altered using the Bruceton staircase test procedure [11]. Twenty to thirty separate tests are conducted at several pulse lengths, and the pulse length required for ignition of 50% of the samples is calculated. This is designated t_{igG}.

Both approaches were examined in this study. However, because of the large number of tests required for the Go/No-Go approach, the time to first light, t_{ig}, was the approach usually adopted.

8

4. Experimental

4.1 Laser

The experiments were carried out using a 400 W CO_2 laser (Coherent Radiation Model 275). The beam diameter at the sample surface was 11 mm which gave a maximum power density of approximately 2000 W cm^{-2} in pulsed mode or 500 W cm^{-2} in CW mode. A schematic of the experimental set-up is shown in Figure 1. Variation in the incident power density was achieved by varying the current through the laser tube. The power density was monitored regularly using a ballistic calorimeter and a power meter. The laser beam pulse length was variable, ranging from 0.01 ms to continuous and was mechanically controlled.

The visible and IR emission from the reacting sample was monitored using a silicon photodiode with a spectral response in the range 400-1150 nm. The output from the diode along with a laser synchronisation pulse were recorded and analysed with a Norland digital storage oscilloscope. The data were also stored on floppy disc for further analysis.

Powdered samples were pressed into standard brass PVU-1A primer cups and placed in a brass holder on a translation stage in a firing box. The laser beam was admitted through a light tight aperture at the top of the firing box and centred onto the sample. Each sample was exposed to a single laser pulse and the result recorded as an ignition or non ignition. To ensure one dimensional heating of the sample, the laser beam diameter was greater than the sample diameter. A glass tube was placed around the sample to minimise convective air currents due to the exhaust system. At least five tests were conducted for each composition at each laser power density level to obtain t_{ig}. The pulse length was set arbitrarily to a value greater than t_{ig} to ensure ignition of the sample. Each sample was tested, on average, at four power density levels: 75 W cm^{-2}, 160 W cm^{-2}, 260 W cm^{-2} and 400 W cm^{-2}. All tests were performed at ambient temperature and pressure.

4.2 Pyrotechnic Compositions

A full list of the compositions studied is given in Tables 1 and 2; these represent a range of pyrotechnics from colored smokes to igniter/ignition compositions, primer compositions and delays. The SK smoke compositions were Canadian (Defence Research Establishment Valcartier) and were supplied as cast slabs; the US series of compositions were US M-18 colored smokes obtained in powder form from CRDEC (Chemical Research Development and Engineering Center, Aberdeen Proving Ground, Maryland); the UK series of compositions were UK L-series colored smokes obtained as powders from Royal Armament Research and Development Establishment, Fort Halstead, UK. All the other compositions were production stocks held at Naval Ordnance Station, Indian Head, Maryland.

The powdered samples (20 mg - 30 mg) were pressed into a brass cup at 73 kg dead load. The cast colored smoke samples were cut from slabs using a cork borer (0.25 cm diameter, approximately 450 mg); the cast Magnesium/Teflon/Viton (MTV) samples were similarly obtained (approximately 100 mg) and the MTV pellets were pre-cut production samples (4-8 mm length, 2-4 mm diameter). All the cut samples were tested with the cut face perpendicular to the incident laser beam.

9

4.3 Laser Beam Characteristics

In any experiment involving lasers, the beam profile must be measured and controlled. The temporal and spatial characteristics of the laser beam were monitored with a fast pyroelectric detector (Barnes Engineering T301 PZT) with a sampling area of $1.00 \, mm^2$. The detector was mounted on the translation stage in place of the sample holder and its output was taken to a digital oscilloscope (Norland 3001). The detector output for two separate orthogonal traverses across the laser beam in the X and Y direction is shown in Figure 2. Figure 2 clearly shows that the detector response is typically Gaussian in shape with no apparent hot spots. The centre of the laser beam is at $X = 0.667$ mm and $Y = 0.950$ mm and it has an almost uniform power distribution. The relationship between the average power density over the test sample and the measured beam power is determined mathematically. The Gaussian beam power is:

$$P(r) = P_o e^{-2r^2/r^{*2}} \tag{1}$$

where P_o = peak power
         r = beam radii
         r^* = $1/e^2$ beam radius

Therefore the power incident on a circle of radius r is:

$$P_r = \int_0^r P(r) \, dA$$

$$= (\pi r^{*2}/2) P_o [1 - e^{-2r^2/r^{*2}}] \tag{2}$$

As $r \to \infty, \; P_\infty \to (\pi r^{*2}/2) P_o \tag{3}$

From equations 2 and 3, the average power density over a sample of radius r is

$$\bar{P} = P_r/\pi r^2 = P_\infty/\pi r^2 (1 - e^{-2r^2/r^{*2}}) \tag{4}$$

Therefore, for the central portion of the beam (0.2 cm), the relationship between measured power and the average power density is $\bar{P}_\infty = 0.518$ P (Fig. 3). In this work, the total beam power was determined with a ballistic calorimeter and the average power density over the sample derived from the calibration graph. These relationships illustrate the importance of the sample size; the smaller the sample diameter, the more uniform the power across the sample. Also, to ensure one dimensional heating of the sample, the sample diameter must be less than the beam diameter. If very small samples are used, then the average power over the sample approximates to the peak power.

5. Results and Discussion

The following sections deal in detail with each type of pyrotechnic material assessed.

5.1 T-10 Delay Composition

Figure 4 shows that, for the T-10 delay composition, the time to ignition decreases as the incident power density increases. From studies of the behaviour of propellants and other pyrotechnics [8, 12, 13], relationship (5) has been found to hold. Figure 4 shows the line of best fit corresponding to this type of relationship for the T-10 delay composition.

$$\log(t_{ig}) = n \log (\text{power density}) - B \tag{5}$$

For T-10, n = -1.4 which is similar to values of -1.5 to -2.0 recorded for propellants and explosives [13]. When the results are converted to ignition energy density using equation 6, a complex relationship between ignition energy density and power density is observed (Fig. 5).

$$\text{Ignition energy density} = (t_{ig}) (\text{Power density}) \tag{6}$$

The important characteristics of Figure 5 are the apparent existence of a critical energy density, E_c and a minimum power density, q_1, that must be supplied to the sample for ignition to occur. The critical energy is equal to $E_c = q_c t_c$ where t_c is the ignition time at the critical power density q_c.

As the power density increases, the ignition energy density decreases rapidly until a minimum (critical) energy density value is reached; further increase in the power density results in a small increase in the ignition energy density. It should be noted that further testing at higher power density levels should be undertaken to confirm whether the slight increase in energy density at high power density levels is a real effect or whether it results from the experimental error.

Figure 5 can be explained in terms of the sample thermal response. As the sample is heated, its thermal conductivity removes heat from the surface into the bulk sample. Heat is also lost through radiation from the sides of the sample although this is significant for only the outer few mm of the sample. If the rate of heat input is less than the rate of heat loss, ignition will not occur. In Figure 5, q_1 represents the minimum rate of radiant heating needed to balance the heat losses and achieve ignition. As the power density increases beyond q_1 the rate of energy delivery to the sample increases, t_{ig} decreases, and the ignition energy density decreases.

This process continues until a critical ignition energy value, E_c, is reached. At this point, the power density is sufficient that the temperature gradient in the sample is very small and there is only a minimal diffusion of heat into the sample before ignition occurs. Increasing the power density has little effect on t_{ig} and consequently, little effect on the energy density.

11

With these high power densities, the physical processes involved in the ignition process (melting, evaporation, boiling etc.) may "outstrip" the actual chemical processes [14]. This would remove a heat feedback source and would necessitate an increase in the energy density. This could explain the small increase in the energy density at the high power density levels as seen in Figure 5.

At very high power density levels, some physical disruption to the sample surface has been observed with explosives and propellants [15, 16]. Any physical modification to the surface (cracking, cratering, ablation, etc.) would effect energy transfer processes and could be a contributing factor to the higher ignition energy density at high power density levels.

Figure 6 shows the change in t_{ig} at four incident laser power densities for T-10 composition pressed at 25-160 kg dead load (20-150 MPa). All the samples showed regular and complete combustion and t_{ig} decreased as the power density increased. As the pressing load and hence the sample density increased, t_{ig} decreased. The decrease in t_{ig} was greater at the lower than the higher power density levels. Although the spread of results is larger than ideal, the trend is apparent.

T-10 is a typical "gasless" delay composition and combustion is assumed to propagate predominantly via conductive heat transfer. As the sample density increases, the thermal conductivity increases and heat flows more readily away from the sample surface into the interior. The mass of material to heat also increases if the volume remains constant. Both these effects are assumed to increase t_{ig}. For example, Johnson [17] developed a theoretical equation for the ignition of pyrotechnics based on a purely thermal model where ignition was deemed to occur when a critical temperature was reached. From this:

$$t_{ig} = k\rho c\, A^2\, F^2\, (T_i - T_a)^2 / \pi q^2_{in}$$

where k is thermal conductivity, ρ is density, c is heat capacity, A is the sample surface area, q_{in} is the heat flow in, T_i is the designated ignition temperature and F is a constant. This equation predicts that as the sample density increases, t_{ig} increases.

Figure 6 shows a quite unexpected behaviour, with t_{ig} decreasing as the sample density increases. The effect is most pronounced at low incident flux densities.

The behaviour shown in Figure 6 has also been observed by Holst [9] for a pyrotechnic tracer composition but no explanation of the behaviour was proposed. Menichelli's [4] results for several explosives and pyrotechnics suggested that t_{ig} increased with sample density but the results were inconclusive. It has also been observed that t_{ig} for lead azide decreases as the pressing load increases [18].

Due to the limited test results no valid conclusion could be drawn for the behaviour of the T-10 composition. However, they do highlight interesting behaviour which will be addressed in detail elsewhere.

5.2 Ignition Compositions

Figure 7 shows the change in t_{ig} with power density for the four ignition compositions; $Zr/KClO_4$, B/KNO_3, A1A and G-11. The ignition response follows the linear relationship in Equation 5 with the time to ignition decreasing as the incident power density increases. The value of n ranges from -1.03 for G-11 to -1.53 for B/KNO_3, which agrees broadly with general propellant ignition theory of $-2.0 < n < 0$ [19]. The different values of n are due to the inherent differences in the thermal and kinetic properties of the compositions (activation energy, specific heat, thermal conductivity, etc.). Figure 8 shows the relationship between the ignition energy density and power density. $BKNO_3$ and ZKP compositions show similar behaviour to that observed for T-10 with a clear critical energy density required for ignition. G-11 and A1A compositions do not show as clear a response as $BKNO_3$ or ZKP but a critical energy density can be determined. Compositions $Zr/KClO_4$ and B/KNO_3 also show the existence of a minimum power density whilst G-11 and A1A do not. In fact, G-11 and A1A exhibit an almost constant ignition energy density, independent of power density.

Table 3 shows that the order of ignition sensitivity (in terms of critical energy density) is A1A > G-11 > B/KNO_3 > $Zr/KClO_4$. Surprisingly, the delay composition T-10 is more sensitive than nearly all the igniter compositions with the exception of composition A1A. Table 3 also presents typical safety/sensitivity data for these ignition compositions [20]. Comparison with the laser critical energy densities shows no obvious relationship between radiant ignition sensitivity and impact sensitivity, spark sensitivity or temperature of ignition.

Examination of the samples after irradiation showed that they had all burnt to completion with the exception of the $Zr/KClO_4$ samples. For $Zr/KClO_4$, sustained combustion could only be achieved infrequently, with often only 20-80% of the sample mass being consumed. Premature termination of combustion occurred predominantly at the lower power density levels; simply increasing the pulse length proportionally increased the amount of sample burnt. Poor combustion may not be simply due to the level of input energy but may be due to the need to confine the $Zr/KClO_4$ composition to ensure sustained combustion. It may also be proposed that the zirconium in the pressed sample enhances the thermal conductivity of the composition causing heat to be conducted away from the reaction front. It is also possible that at ambient pressure the gaseous decomposition products (approximately 50% w/w of total products in gas phase) move away from the reaction surface, decreasing the heat transferred back to the unreacted sample and thereby causing ignition failure.

Figures 9(a) and 9(b) show typical oscilloscope records for the ignition of two identical samples of $Zr/KClO_4$. Figure 9(a) shows sustained combustion of the sample beyond the termination of the laser pulse but that the light output decreased when the laser pulse terminated. Approximately 80% of the sample had burnt. The decrease in the light output is most probably due to a reduction in the sample burn rate with the removal of the external heat source. Figure 9(b) shows a photodiode response (first light output) 97.5 ms after being exposed to the incident laser pulse. On the basis of the definition of t_{ig}, the sample ignited after 97.5 ms, but the progression from ignition to complete combustion could not be achieved as recorded by the termination of the light output from the sample after approximately 155 ms. Note that complete combustion could not be achieved even with continued laser heating. The sample showed some slight blackening on the top surface only. These results suggest that the experimental arrangement has not been optimised for the laser ignition of these compositions.

13

The G-11 composition also exhibited irregular light output at low power density levels and a reduction in light output on termination of the laser pulse. However, complete combustion of the sample always occurred.

5.3 SK, US, and UK Smoke Compositions

The colored smoke compositions comprised both pressed powder (US and UK) and cast samples (SK series). Figures 10, 11, 12 show the change in t_{ig} with power density for the SK, US and UK compositions respectively and Table 4 presents critical ignition density results and standard sensitivity data (ignition temperature, DSC/DTA, etc.) [21].

Direct laser ignition of several colored smoke compositions was demonstrated but the transition from ignition to sustained combustion appears to be very difficult to achieve even if high laser flux levels are used and the pulse length is long. At low flux levels, the combustion process was very erratic and increasing the laser pulse length simply increased the combustion time in direct proportion to the increase in the laser pulse length. Complete combustion did not occur for any of the samples examined.

Figures 10, 11 and 12 show that the ʻmoke composition responses again follow the linear relationship in Equation 5. The values of n again fall within the expected range $(0 > n > -2)$ with a high of -0.7 for USY to -1.3 for USV. The spread of the results is somewhat less than ideal and the correlation coefficient of the "line of best fit" was sometimes as low as 0.8. This behaviour is probably due to the small number of samples tested and the variable nature of the ignition process and the transition from ignition to combustion.

Figure 13 shows a typical oscilloscope recording for UKB smoke composition and illustrates the problem of ignition (note period of unstable reaction before ignition commenced) and maintenance of combustion (combustion continued only as long as the laser pulse was on). This behaviour was confirmed visually with often little more than 20% of the sample mass being completely burnt. Increasing the laser pulse length simply increased the combustion time proportionally. However, increasing the power density sometimes ensured that combustion continued after termination of the laser pulse.

Figure 14 shows the oscilloscope recording for SK338 smoke composition. In this case, the sample showed none of the transient combustion behaviour observed for UKB. However, combustion ceased on termination of the laser pulse. This behaviour was followed for almost all the smoke compositions and determination of "ignition" required the sample to be visually inspected.

The US and the UK smoke compositions are in current military use but, as far as the authors are aware, have not exhibited combustion problems of the frequency found here. It is possible that the behaviour of the compositions could have been affected by the low density, low confinement, small mass or small diameter of the sample. If the latter is important, it would suggest that there is a critical diameter for ignition and combustion.

From the results in Table 4, the critical energy densities lie in the range 3-5 J cm^{-2} with the exception of the USV composition. The formulation of USV (Table 1) is not significantly different to the rest of the US smoke compositions and no reason for the result is apparent. Except for the organic dyes used in their formulations, USR and USV compositions are very similar. It is possible that the observed large differences in critical ignition energy densities are due to differences in hygroscopicity leading to

14

moisture absorption. McIntyre [22] provides data showing that a smoke composition similar to USV had a hygroscopicity of 26% at 95% RH whilst a composition similar to USR had only 3.5% at 95% RH. It is possible to propose that the USV sample absorbed moisture during either manufacture or during handling/preparation/testing, which resulted in significantly decreased sensitivity as reflected in the large critical laser ignition energy density. Unfortunately it was not possible to measure the hygroscopicity of the USV and USR compositions in the present work.

Comparison of the laser data with standard sensitivity/safety test data is also shown in Table 4. The laser critical ignition energy data again show no correlation with the Ignition DTA/DSC and Temperature of Ignition data. Perhaps this result is not surprising as the laser has a purely radiant output compared with the conductive and/or convective and/or radiant output associated with the other sensitivity/safety tests. Barton et al [23] showed that the temperature of ignition (DSC exotherm) was related to heating rate (and so energy deposition rate). Since the laser produces a significantly greater heating rate, by at least one order of magnitude, than the safety test methods, this may account for some of the observed differences between the laser data and the sensitivity data.

Thermal initiation of smoke compositions is easier than thermal initiation of ignition compositions due to the low melting points of their fuel (lactose, sulphur) and oxidant (potassium chlorate) which result in lower temperatures of ignition. The laser critical ignition energy density data given in Tables 3 and 4 shows the reverse effect with the ignition compositions recording slightly lower critical energy density figures than the smoke compositions. This result may reflect experimental uncertainty or, at the large heating rates achieved with the laser, the differences in ignition sensitivity between the two groups of pyrotechnics may be significantly reduced.

5.4 Magnesium/Teflon/Viton (MTV)

MTV is a frequently used composition in solid propellant rocket motor igniters. Type II and Type III MTV (see Table 2) were examined as both powder and extruded pellets. An MTV formulation used in the Sidewinder igniter was also examined. Figure 15 presents results for t_{ig} versus power density for all the MTV samples. Even allowing for the scatter of results, differences between the three types of MTV and between the powder and pellet are apparent.

Figure 15 shows that as the laser power density increases, the difference between the values of t_{ig} for the various MTV samples decreases. This is reflected in the variation in n (see Equation 5), the slope of the t_{ig} vs power density line, which has values from -1.2 to -1.3 for all samples except -1.8 for Type II pellets. This suggests that at high power density levels, the effect of differences in sample properties (thermal conductivity, heat capacity, particle size, etc.) becomes negligible. As the power density increases, a steeper temperature gradient is formed and ignition occurs closer to the surface than at low power density levels. Consequently, the samples tend to converge to a similar t_{ig} value at high power density levels.

Differences between the ignition response of the different MTV samples is not unexpected given the particle size and surface area of the different magnesium powders used (see Footnotes 2, 3 & 5, Table 1). Generally, a reduction in particle size of either the fuel or the oxidant leads to a reduction in the time to ignition of the composition. The surface area of the magnesium in Type III MTV is almost ten times greater than that of the magnesium in Type II MTV [24]. The Sidewinder magnesium is similar to that used in Type II MTV, but it has a greater proportion of fines (< 44 μm). Magnesium used in Type III MTV has the largest particle size and hence smallest surface area. Also, the thickness of the viton coating on the

15

magnesium particles will be inversely proportional to the surface area of the magnesium, and the thinner the viton coating, the greater the ignitability of the MTV. Consequently, the order of ignition response would be expected to be Type III MTV > Sidewinder > Type II MTV. Figure 14 confirms this result for the MTV pellets but shows little difference between the value of t_{ig} for Type II and Type III MTV powders.

Table 5 presents the critical energy density data for all the MTV compositions. The difference between the compositions is relatively small with < 10% difference between the "most" ignitable and the "least" ignitable MTVs. Comparison of these data with Tables 3 and 4 shows that MTV is less ignitable than all the igniter compositions and the colored smoke compositions.

Examination of the oscilloscope traces for the MTV samples shows some interesting features. All the MTV samples show erratic pre-ignition behaviour (Fig. 16). The existence of multiple light output peaks suggests that several reactive sites form on the sample surface before ignition and sustained combustion occur. Figure 17 is an enlargement of the pre-ignition behaviour shown in Figure 16 and clearly shows numerous active reactions (light outputs) on the sample surface before combustion occurs. Habersat [25] has noted that on irradiation there is often a rapid change in the intensity of the visible light emitted before steady state combustion commences. There may be several of these "quick-rises" which can lead to marginal ignition.

Once ignited, most of the samples burnt completely although the Type II MTV pellets often ceased combustion on termination of the laser pulse. Several instances of "dynamic extinction" were observed; combustion was achieved but then ceased some time after the laser was terminated, leaving unburnt sample behind. This behaviour has been observed for several energetic materials [26] and is thought to be due to the loss of energy and reduced heat transfer to the surface of the material due to the movement of the reacting gases away from the sample surface.

The orientation of the MTV pellets was altered to examine the effect of pellet curvature on t_{ig}. The previous tests were conducted with the pellet flat face perpendicular to the incident laser beam. Several tests were conducted with the pellet horizontal, i.e. the curved portion exposed to the laser beam. Figure 18 and Table 5 show that there is little difference between the samples tested.

The Sidewinder MTV samples were cut from a single cast slab in a similar manner to the cast colored smoke compositions. The pellets were then cut in half exposing an "internal" MTV face which had been unexposed since manufacture. A previous study had shown the external surface to have a shorter t_{ig} than the internal surface [10]. We re-examined this and Figure 19 shows that, for the samples used, there is little difference between the ignitability of the two surfaces although the external surface shows lower values of t_{ig} at low power density levels than the internal surface samples.

5.5 Effect of Formulation Variation

Lasers have been proposed as a means of conducting routine ignitability tests on pyrotechnics for quality control purposes. However, little data is available on the sensitivity of the system to small variations in the pyrotechnic formulation. A group of compositions was chosen to examine the effect of small changes in the formulation on t_{ig} and E_c. The formulations are shown in Table 6; within each group, the proportion of the fuel was increased or reduced by 5% and 10%, and the oxidant changed accordingly. Figure 19 shows the change in t_{ig} with

16

power density for the composition. The spread of experimental data is certainly less than ideal, but there is a clear change in t_{ig} values with formulation changes; reducing either the fuel or oxidant reduces t_{ig}. The critical energy density values for the compositions show a similar behaviour (Table 6); reducing either the fuel or the oxidant reduces the critical energy density.

Formulation 1-Z1 is a standard US igniter composition. The choice of pyrotechnic formulations generally depends on performance parameters such as heat of reaction, brisance of output, burn rate etc. This result suggests that the standard formulation is also the least ignitable, and highlights that only minor changes in the formulation are sufficient to increase its radiant ignition sensitivity.

The oscilloscope recordings showed that composition 1-Z1 ceased combustion on termination of the laser pulse (Fig. 20 (a)) and examination of the sample showed extensive unburnt material remaining. Complete combustion occurred for all the other samples. Figures 20(b) and 20(c) show the oscilloscope recordings for 1-Z2 and 1-Z3 respectively. The time base for this data is identical, however the time of light output for 1-Z3 is significantly greater than that for 1-Z2. Since both samples burnt to completion, the result indicates a change in the burn rate with a change in the percentage fuel. This result is not unexpected but does suggest that this technique may be used to measure the burn rate of pyrotechnic samples.

5.6 Ignition Criteria

Using the two different definitions of the time to ignition as discussed in Section 4 (t_{ig} and t_{igG}), samples of T-10 delay composition were tested and the results compared. Using the Go/No-Go approach, the pulse length necessary to ensure ignition will always be greater than or equal to t_{ig}.

Figure 21 shows that there is a small difference between the two results with the time to first light (t_{ig}) giving the longer times to ignition. It is possible that the results are not significantly different due to experimental uncertainty. The Go/No-Go tests were conducted several months after the "first light" experiments and after a period of extensive laser repair. The most reasonable explanation of these results was that there was a shift in the calibration of the laser.

Additional testing after laser calibration with A1A compositition showed that the energy densities derived using the Bruceton procedure are greater than those from the oscilloscope recordings (see Section 6.7) as expected.

Discounting the discrepancy, the time to first light is generally the preferred method. The time taken to obtain a result with the Go/No-Go method is significantly greater because of the larger number of tests required; 30-50 tests at each power density level for Go/No-Go compared to 5-10 for time to first light.

5.7 Ignition Energy and Ignition Power

Figure 5 illustrated that composition T-10 exhibited a critical ignition energy density and also a minimum power density for ignition. This relationship was further examined in a series of tests using the ignition composition A1A. The power density was pre-set and the pulse

17

length varied using a Bruceton test plan to determine the pulse length for 50% ignition (t_{igG}). The time to ignition (t_{ig}) measured from the oscilloscope records was also determined.

Figure 22 shows the relationship between the Bruceton energy density (energy density = $t_{igG} \times$ power density) and the Bruceton pulse length. For this range of pulse lengths, the power density is constant whilst the energy density increases linearly. Figure 23 shows the change in power density with energy density. As the energy density for ignition increases (long pulse length) the power density approaches a minimum value. Similarly, as the power density increases (short pulse length), the energy density approaches a critical value for ignition to occur. The results for both Bruceton and "first-light" methods agree closely, and as expected the energy densities derived using the Bruceton procedure are slightly greater than those from the oscilloscope recordings.

The existence of a critical energy density and a critical power density was examined by Oestmark [6] for a Mg/NaNO$_3$ composition; he proposed that for long duration of energy input, the composition was characterised by a threshold ignition power whilst for short duration of energy input, the composition was characterised by a threshold ignition energy density. The results reported here for T-10 tend to support this general theory, but the range of pulse lengths used was not sufficient to cover the constant power density region with a large degree of confidence.

5.8 Effect of Laser Pulse Length

One of the experimental variables that is frequently not examined is the effect of the incident laser pulse length on the time to ignition. This is not unreasonable as it is assumed that as long as the incident pulse length is greater than t_{ig}, then the two variables should be independent. Figure 24 presents the results of an examination of the effect of pulse length on t_{ig} at a range of power density levels for A!A composition. For the power density levels examined, the time to ignition is not independent of the pulse length, and it appears to increase linearly as the pulse length increases. However, the increase in t_{ig} is small and may not be significant given the experimental uncertainty. This result is still important as it implies that comparison between any groups of samples should be conducted with a knowledge of the pulse length of the incident radiation used and corrections may need to be applied.

Figure 24 suggests a possible systematic change in the time to ignition with pulse length. No logical explanation can be offered for this behavior other than errors in the experimental apparatus (variation in the power density with pulse length, or a change in the laser beam energy profile with pulse length etc) or experimental procedure. The pulse length was electronically checked every 2 to 3 pulses and verified with the oscilloscope recording. No evaluation of the power density pulse length/beam profile was possible and further analysis is warranted.

6. Conclusions

Laser ignition is a well defined and readily quantified tool that may be used to study the ignition of pyrotechnics. It offers the advantage in the ability to control and measure the radiant energy input into the pyrotechnic material. This work has shown that a range of

18

pyrotechnic compositions may be initiated successfully given the correct conditions (e.g. pulse length, incident energy, sample density, power density, particle size) and that the dependence of the ignition energy on these parameters can be easily determined. However, the transition from ignition to complete combustion was difficult to achieve with some compositions and the effect of sample confinement needs to be examined.

This laser technique confirms that for long duration irradiation, ignition is characterised by a minimum power density level and as the pulse length decreases, ignition becomes characterised by a critical energy density. All the pyrotechnics examined exhibit similar critical energy densities (1-4 J cm^{-2}) with the exception of MTV ignition composition (13 J cm^{-2}).

With current high power laser diodes, these critical ignition energy densities are not difficult to obtain. Consequently, the development of a practical laser initiation system for pyrotechnics is possible.

The use of the light output from the reacting pyrotechnic may provide useful information on pre-ignition reactions and burn rate of the compositions. Surface reactions also appear to be important in the ignition process, especially at high power density levels and short pulse lengths. Comparison between laser ignition data and that from other non-radiant ignition sources can yield useful insights into the ignition behavior of pyrotechnics but the effect of differences in the type of ignition source should be kept in mind.

7. Acknowledgements

8. References

1.   Brich, A.A., Galeeve, I.A., Zaitsev, B.N., Sbitnev, E.A. and Tarinstev, L.V. (1969). Mechanism of initiation of condensed explosives, *Fizica Goreniya Vzyva*, 5 (4), 457.

2.   Ostrowski, P.P. and Grant, J.F. (1981). Laser ignition characteristics of M-26 gun propellant. *18th JANNAF Combustion Meeting*, Jet Propulsion Laboratory, Pasadena, CA, USA, p. 55.

3.   DeLuca, L., Ohlemiller, T.J., Caveny, L.H. and Summerfield, M. (1976). Radiative ignition of double based propellants. *AIAA Journal*, 14, 7.

4.   Menichelli, V.J. and Yang, L.C. (1970). *Sensitivity of explosives to laser energy* (TR-32-1474). Pasadena, CA: National Aeronautics and Space Administration, Jet Propulsion Laboratory.

5.   Yang, L.C. and Menichelli, V.J. (1971).   Detonation of insensitive high explosives by a Q-switched ruby laser.   *Applied Physics Letters*, **19** (11), 473.

6.   Oestmark, H. (1985).   Laser as a tool in sensitivity testing of explosives. *Proceedings of 8th Symposium (International) on Detonation*, Albuquerque, NM, USA, p. 473.

7.   Oestmark, H. (1987).   Laser ignition of explosives : ignition energy dependence of particle size.   *Proceedings of 12th International Pyrotechnics Seminar*, Juan-les-Pins, France, p. 241.

8.   Chow, C.T. and Mohler, J.M. (1987).   Thermal ignition of pyrotechnics with lasers. *Proceedings of 12th International Pyrotechnics Seminar*, Juan-les-Pins, France, p. 55. 9.

9.   Holst, G.C. (1979).   Laboratory ignition of artillery tracers.   *Journal of Ballistics*, **3** (4), 627.

10.   Gebhard, T. (1988).   Naval Ordnance Station, Indian Head, USA, private communication.

11.   Culling, M.P. (1953).   *Statistical methods appropriate for evaluation of fuze explosive train safety and reliability* (NAVORD Report 2101).   Whiteoak, MD: US Naval Ordnance Laboratory.

12.   Baer, A.D. and Ryan, N.W. (1965).   Ignition of composite propellants by low radiant fluxes. *AIAA Journal*, **3**(5), 884-889.

13.   Kuo, K. and Summerfield, M. (ed.) (1984).   Fundamentals of solid propellant combustion.   *Progress in Astronautics and Aeronautics*, **90**, AIAA, New York, USA.

14.   Siddiqui, K. and Smith, I. (1974).   The ignition of double based propellants by hot particles arising in the igniter products. *Proceedings of 10th AIAA/SAE Propulsion Conference*, CA, USA, p. 1.

15.   Tang, T.B., Chaudhri, M.M., Rees, C.S. and Mullock, S.J. (1987).   Decomposition of solid explosives by laser irradiation : a mass spectrometric study.   *Journal of Materials Science*, **22**, 1037.

16.   Ostrowski, P.P., Grant, J.F. and Downs, D.S. (1981).   Laser ignition characteristics of M-26 gun propellant. *Proceedings of 18th JANNAF Combustion Meeting*, JPL, USA.

17.   Johnson, D.M. (1965). *Ignition theory: application to the design of new ignition systems* (RDTR-56).   Crane, IN: US Naval Ammunition Depot.

18.   Aleksandrov, E. and Tsipilev, V. (1982).   Effect of pressing pressure on the sensitivity of lead azide to the action of laser radiation.   *Combustion, Explosives and Shock Waves*, **18**, 215.

19.   Merzhanov, A.G. and Averson, A.E. (1971).   The present state of the thermal ignition theory : an invited review.   *Combustion and Flame*, **16**, 89-124.

20. Potter, L.J. and Valenta, F.J. (1989). Comparison of several pyrotechnic compositions of interest at Naval Ordnance Station. *Proceedings of the 4th Congres International de Pyrotechnie du Groupe de Travail de Pyrotechnie,* La Grand-Motte, France, p. 77.

21. Barnes, P., de Yong, L., Domanico, J., Twardawa, P. and Valenta, F. (1987). *A comparison between several standard methods used to characterise the ignition/ignition transfer of pyrotechnic compositions - a collaborative study. Part 1 : Data* (MRL Report MRL-R-1043). Maribyrnong, Vic: Materials Research Laboratory.

22. McIntyre, F.L. (1980). *A compilation of hazard and test data for pyrotechnic compositions* (ARLCD-CR-80047). New Jersey: US Army Armament Research and Development Command, Large Calibre Weapon Systems Laboratory.

23. Barton, T., Williams, N., Charsley, E., Ramsay, J. and Ottoway, M. (1982). Factors affecting the ignition temperature of pyrotechnics. *Proceedings of 8th International Pyrotechnics Seminar,* Steamboat Springs, CO, USA, p. 99.

24. Potter, L.J. (1988). Magnesium, teflon, viton igniter sensitivity investigation results. *Proceedings of the 13th International Pyrotechnics Seminar,* Grand Junction, CO, USA, p. 639.

25. Habersat, J. (1981). A method for absolute hazard ranking of energetic materials. *JANNAF Safety and Environmental Protection Sub-committee Meeting,* Kennedy Space Center, Orlando, FL, USA, p. 13.

26. Ostrowski, P., Dabora, E. and Downs, D. (1979). Laser ignition of black powder. *Proceedings of 16th JANNAF Combustion Meeting,* Monterey, CA, USA, p. 499.

Table 1   Formulation of Pyrotechnic Smoke Compositions - Percent by Weight

Chemical	SK Smokes			US Smokes				UK Smokes			
	SK338	SK354	SK356	USV	USG	USY	USR	UK 1	UK 2	UK 3	UK 4
Dye	41.0	46.0	30.0	42.0	32.0	14.0	40.0	32.0	48.0	47.0	46.0
Potassium Chlorate	25.0	23.50	38.0	25.0	27.0	20.0	26.0	30.0	26.0	25.0	26.0
Sodium Bicarbonate	6.0	2.25	2.0	24.0	22.6	33.0	25.0	-	-	-	-
Lactose	-	8.45	12.0	-	-	-	-	29.0	23.0	25.0	25.0
Sulphur	8.0	-	-	9.0	10.4	8.5	9.0	-	-	-	-
Binder	20.0	18.0	18.0	-	-	-	-	-	-	-	-
Benzanthrone				-	8.0	24.5	-	-	-	-	-
Kaolin								2.0	-	-	-
Zinc Oxide									3.0	3.0	3.0

Table 2   Formulation of Pyrotechnic Compositions - Percent by Weight

Chemical	Delay T-10	MTV			Igniter			
		Type II	Type III	Sidewinder[4]	A1A	ZKP	BKNO$_3$	G-11
Boron	3.5						23.7	
Barium Chromate	96.5							
Magnesium		53.5[2]	54.0[3]	54.0[5]				
Teflon		30.7	30.0	30.0				
Viton[1]		15.8	16.0	16.0				
Zirconium					65.0	46.5		
Iron Oxide					25.0			
Diatomaceous Earth					10.0			
Potassium Perchlorate						52.5		
Graphite						1.0		
Potassium Nitrate							70.7	
Laminac Resin							5.6	
Potassium Chlorate								51.0
Antimony Sulphide								26.0
Calcium Silicide								13.0
TACOT								10.0

1. Vinylidene Fluoride and Hexafluoropropylene co-polymer

2. Type II Mg, Granular Mg chips, Granulation 16 (100% thru 150 μm, < 40% retained 75 μm, < 50% pass 44 μm sieve)

3. Type III Mg, Atomised Mg spheres, > 90% pass 44 μm sieve

4. WS 1620A, Ignition grain for Sidewinder igniter

5. Type II Mg, Granular Mg chips, Granulation 16 (100% thru 150 μm, 50-55% < 44 μm sieve)

Table 3   Ignition Sensitivity of Ignition Compositions

Composition	Laser Critical Energy Density (J cm^{-2})	Temperature of Ignition (K)[1]	Impact Sensitivity (mm)[2]	Electrostatic Sensitivity (J)
A1A	1.2	> 673	> 600	< 0.0005
T-10	1.7	> 673	> 600	0.125
G-11	2.3	673	250	0.375
B/KNO$_3$	3.0	> 673	300	1.00
Zr/KClO$_4$	3.3	> 673	475	< 0.0025

1. At constant heating rate of 10 K min^{-1}

2. 5 kg weight, 20 mg sample

Table 4   Critical Ignition Data for Colored Smoke Compositions

Composition	Laser Critical Ignition Energy Density (J cm^{-2})	Ignition DTA/DSC[1] (K)	F of I[2]	Temp of Ignition[3] (K)
SK 354	4.9	615	-	> 623
SK 338	3.7	499	-	585
SK 356	3.9	502	-	609
USV	11.9	515	180	503
USG	4.0	472	130	471
USY	2.5	489	150	445
USR	3.1	508	120	449
UKB	3.1	483	> 200	467
UKG	3.1	491	> 200	473
UKO	3.8	481	> 200	467
UKR	3.9	503	> 200	469

1. Temperature of principal exothermic response (temp. of ignition), heating rate 10 K min^{-1}

2. Figure of Insensitiveness (RDX = 80)

3. At constant heating rate of 10 K min^{-1} using a Woods metal bath

4. Ignition DTA/DSC, F of I and Temp. of Ignition from [21].

Table 5   Critical Ignition Energy Data for MTV Composition

Composition	Critical Ignition Energy Density (J cm^{-2})
Type II, Vertical Pellet	13.2
Type II, Horizontal Pellet	13.0
Type II, Powder	12.4
Type III, Horizontal Pellet	13.0
Type III, Powder	13.8
Sidewinder, External Surface	12.7
Sidewinder, Internal Surface	13.0

Table 6   Formulations and Critical Ignition Energy for Pyrotechnic Compositions

Formulation Designation	Chemical – % by Weight			Comments	Critical Energy Density (J cm^{-2})
	Zr	KClO$_4$	Graphite		
1-Z1	46.50	52.50	1.0	Standard	1.00
1-Z2	44.20	54.80	1.0	Fuel reduced 5%	0.78
1-Z3	41.85	57.15	1.0	Fuel reduced 10%	0.75
1-Z4	49.10	49.90	1.0	Fuel increased 5%	0.86
1-Z5	51.75	47.25	1.0	Fuel increased 10%	0.79
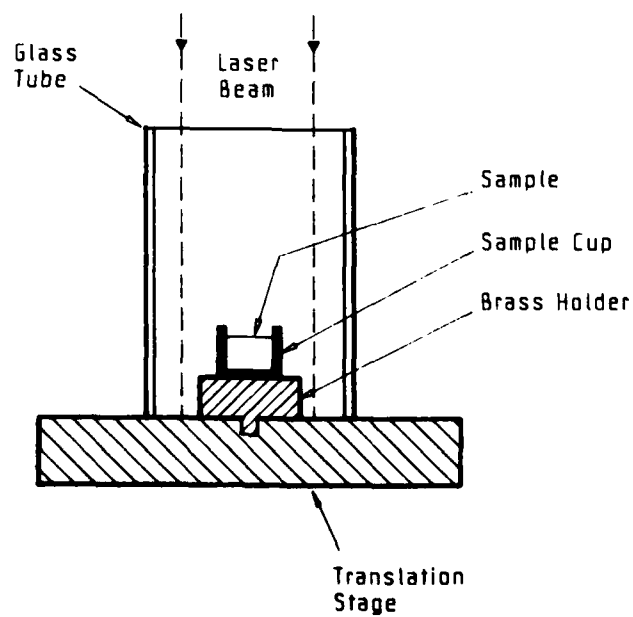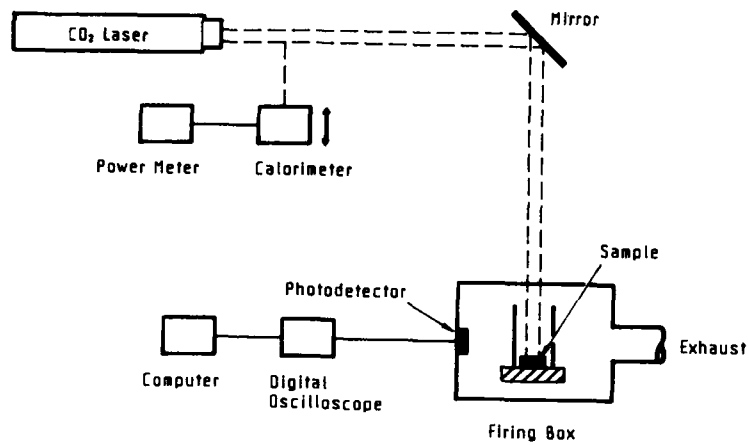
Figure 1   Experimental Arrangement
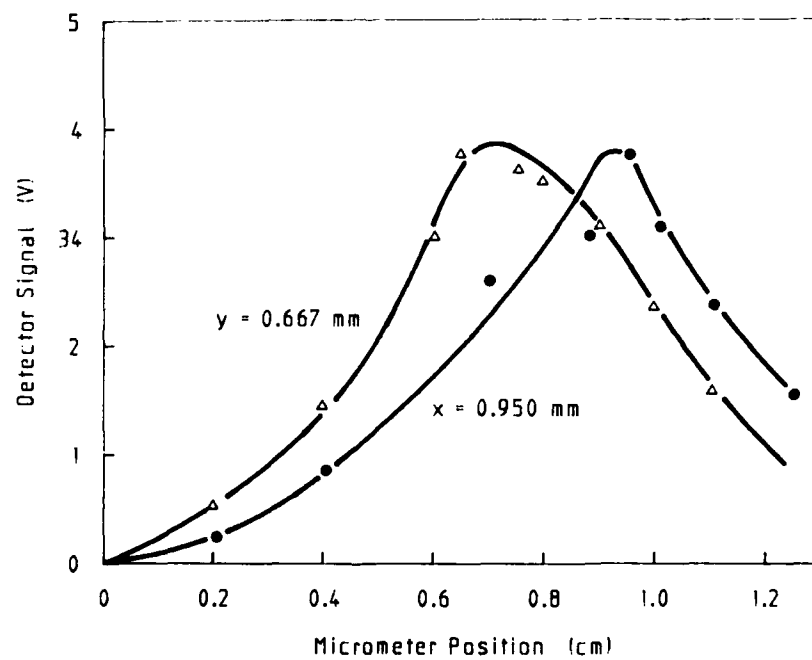
Figure 2   Relative Power versus Position in the Laser Beam
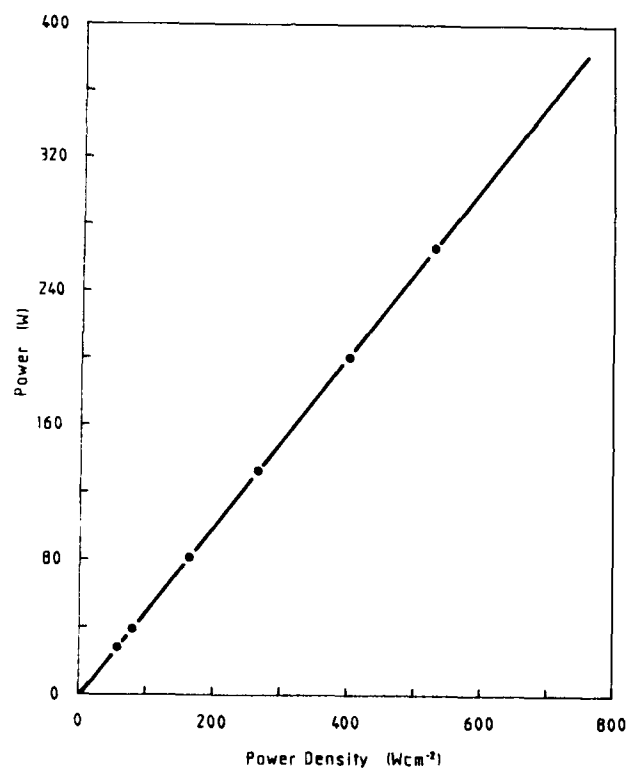
Figure 3   Calibration Curve for Laser Power Density
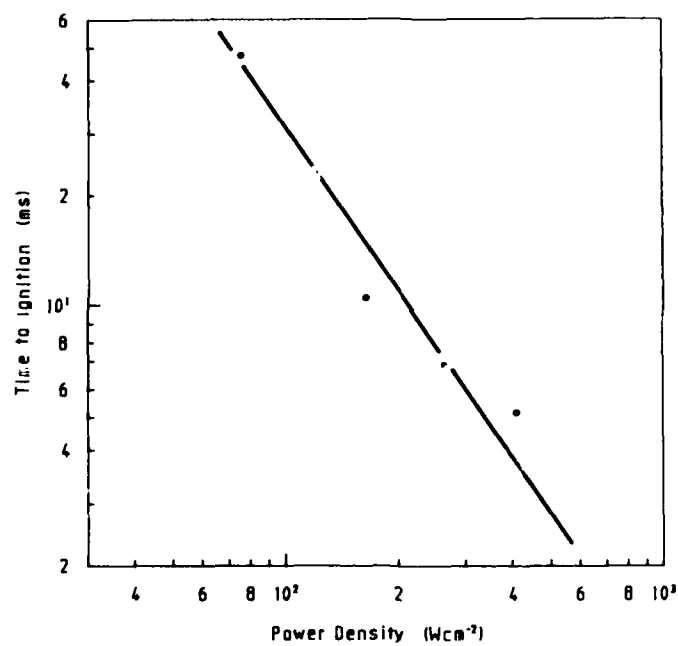
Figure 4 *Relationship between time to ignition, t_{ig}, and laser power density for T-10 delay composition.*
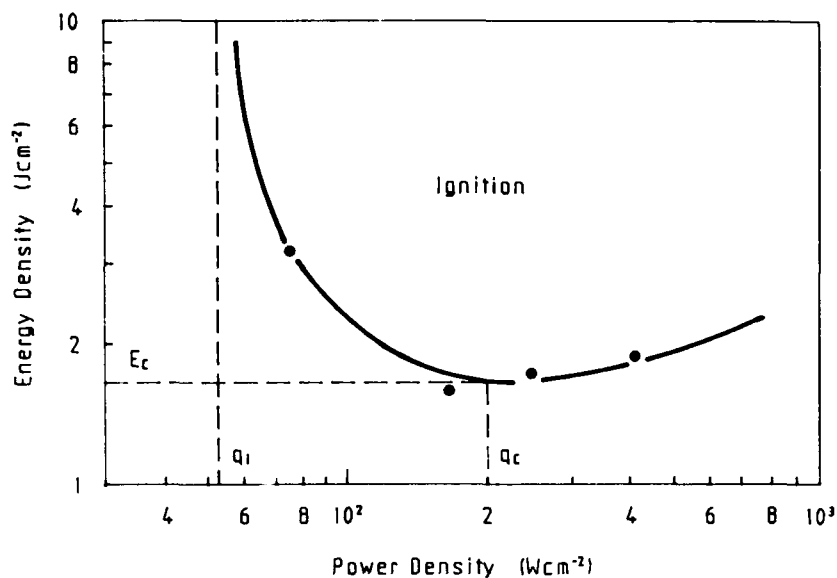
Figure 5   *Relationship between Ignition Energy Density and Power Density for T-10 Delay Composition*
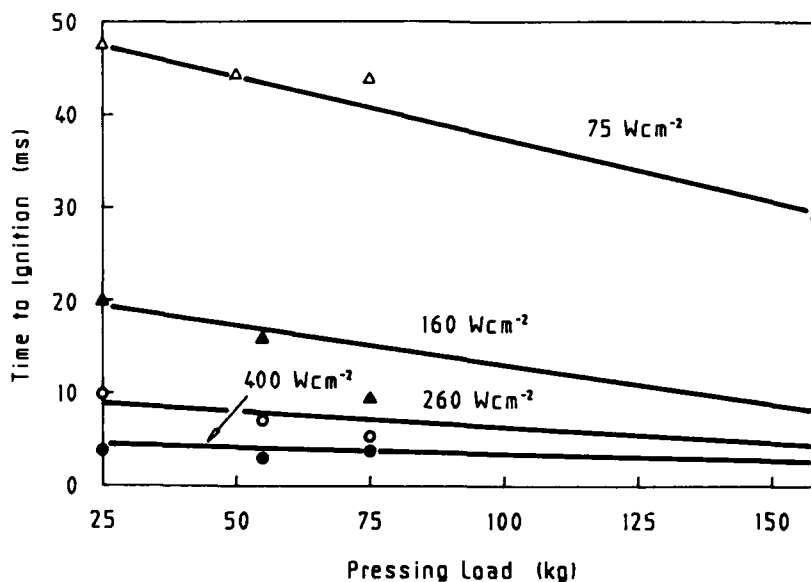
Figure 6   *Effect of Pressing Load on Time to Ignition for T-10 Delay Composition at four incident power densities as shown.*

29

5% and 10%, and the oxidant changed accordingly. Figure 19 shows the change in t_{ig} with

16
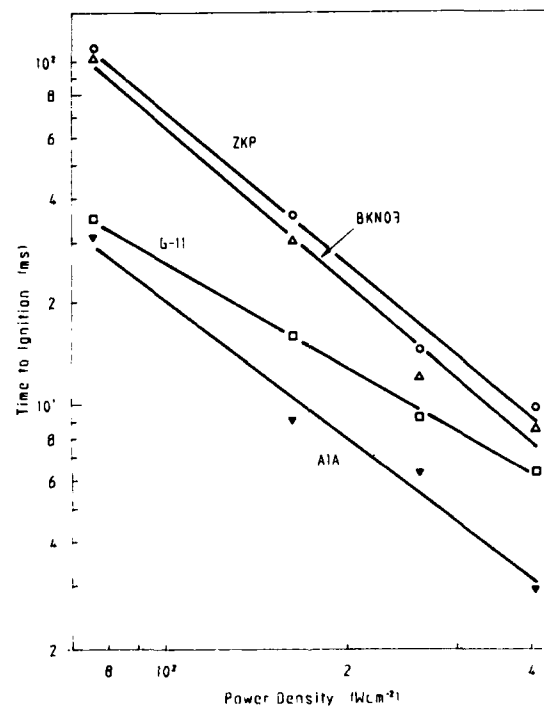
Figure 7   *Relationship between the Time to Ignition and the Incident Laser Power Density for several pyrotechnic ignition compositions.*
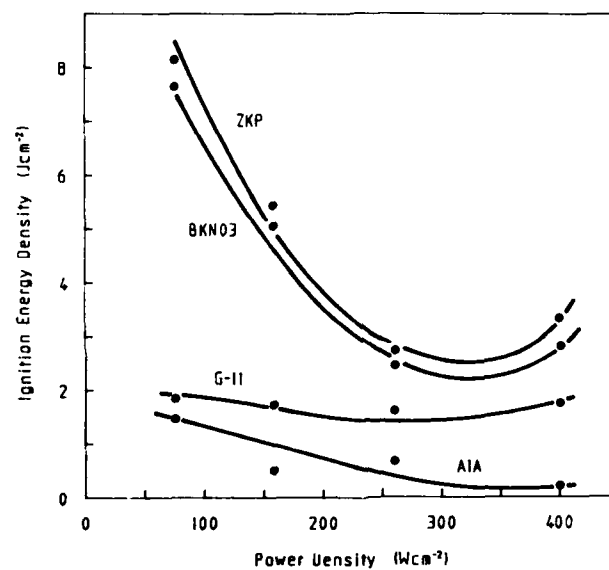
Figure 8   *Variation in Ignition Energy Density with Incident Laser Power Density for several pyrotechnic ignition compositions.*

31
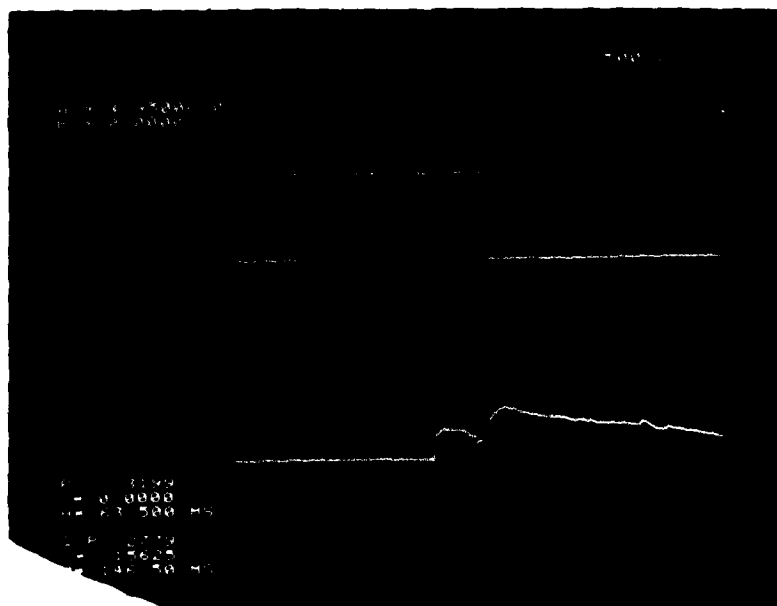
(a)
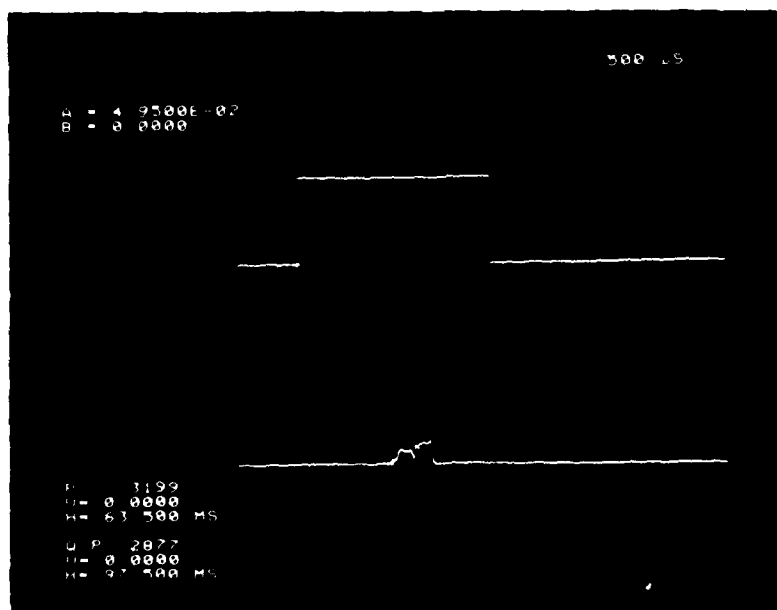
(b)

Figure 9   *Typical Oscilloscope Output for Pyrotechnic Ignition Composition*
Zr/KClO$_4$ (ZKP) at an Incident Power Density of 75 W cm^{-2}. The upper
trace is the laser pulse and the lower trace is the photodiode response.

32
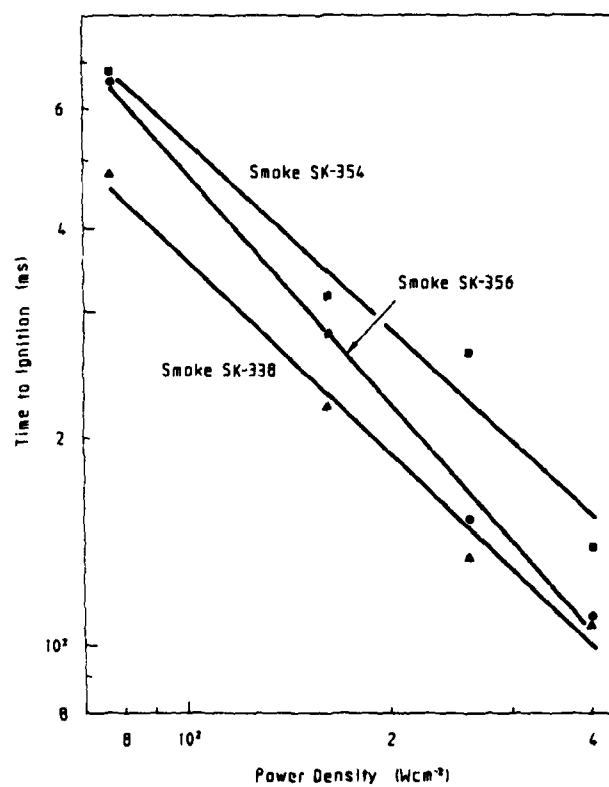
Figure 10 *Relationship between Power Density and Time to Ignition for SK Series of Colored Smoke Compositions.*

33
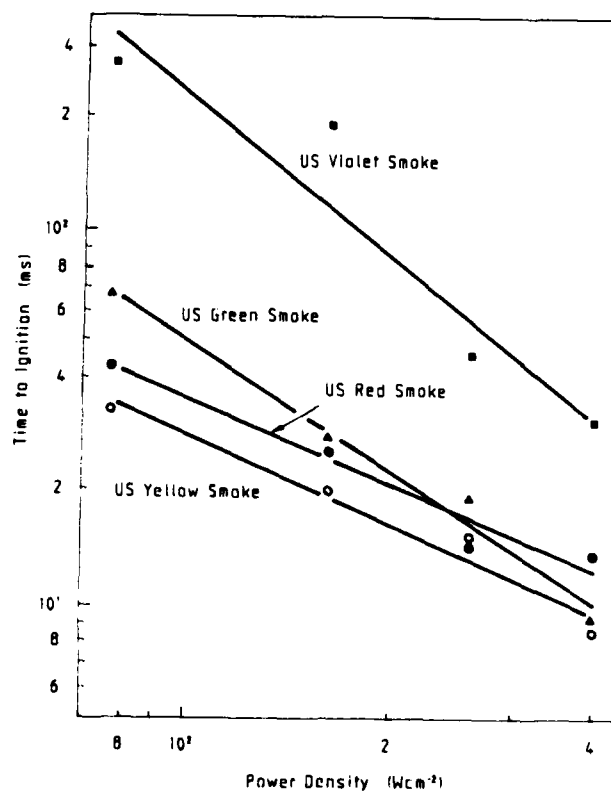
Figure 11   Relationship between Power Density and Time to Ignition for US Series
of Colored Smoke Compositions.
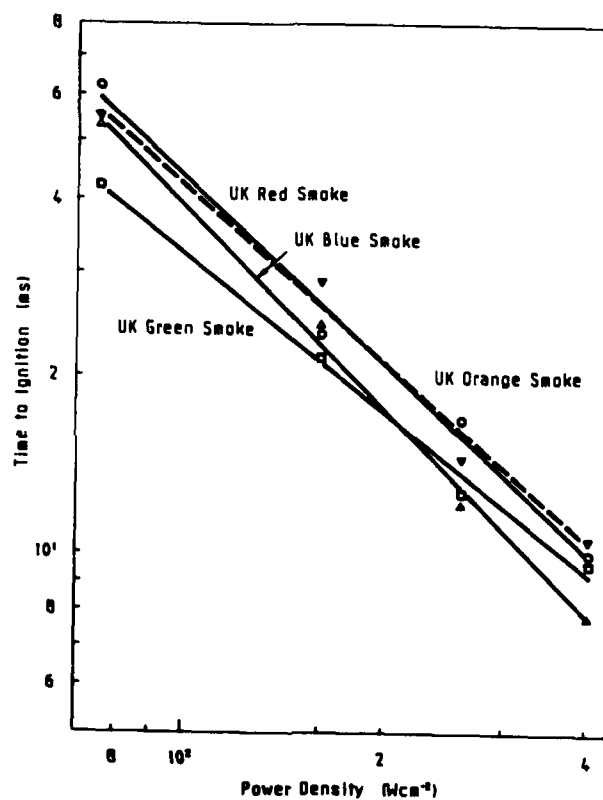
Figure 12   *Relationship between Laser Power Density and Time to Ignition for*
UK Series of Colored Smoke Compositions.
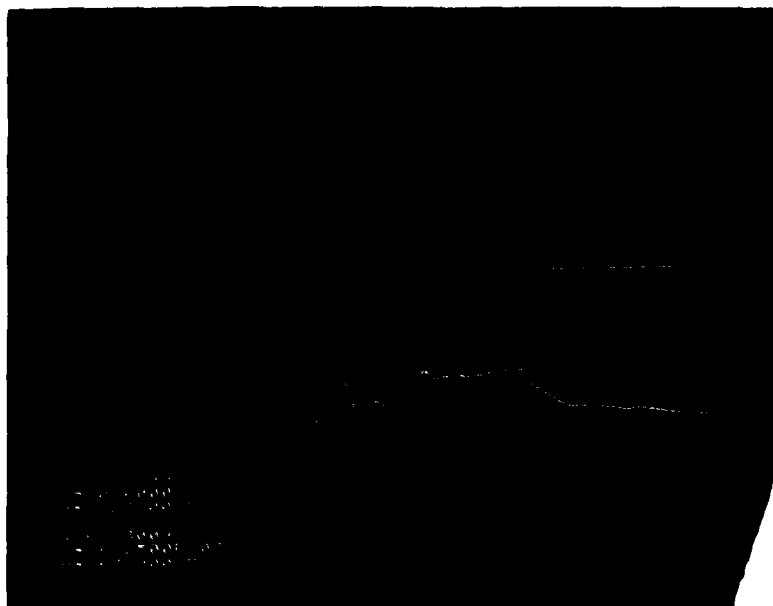
Figure 13   Oscilloscope Response for UK Blue Smoke Composition at Power Density of 75 W cm^{-2}
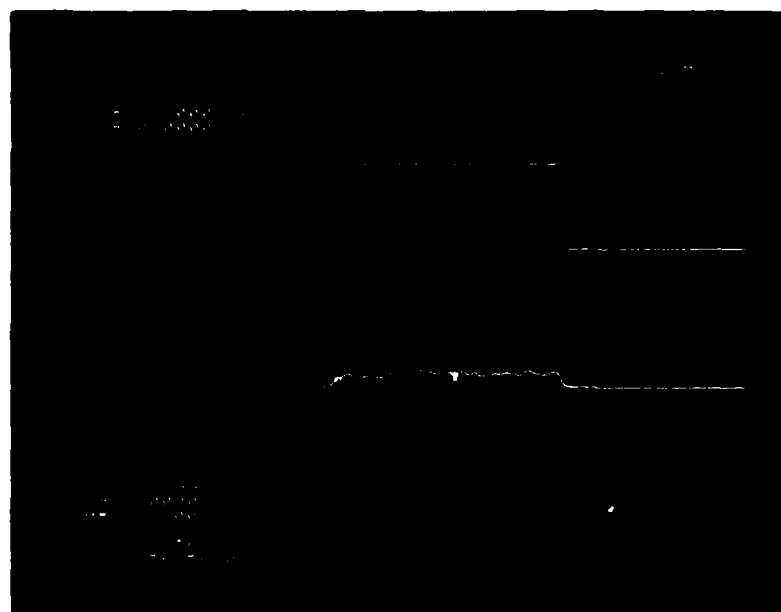
Figure 14   Oscilloscope Response for SK 338 Colored Smoke Composition at Power Density of 160 W cm^{-2}.
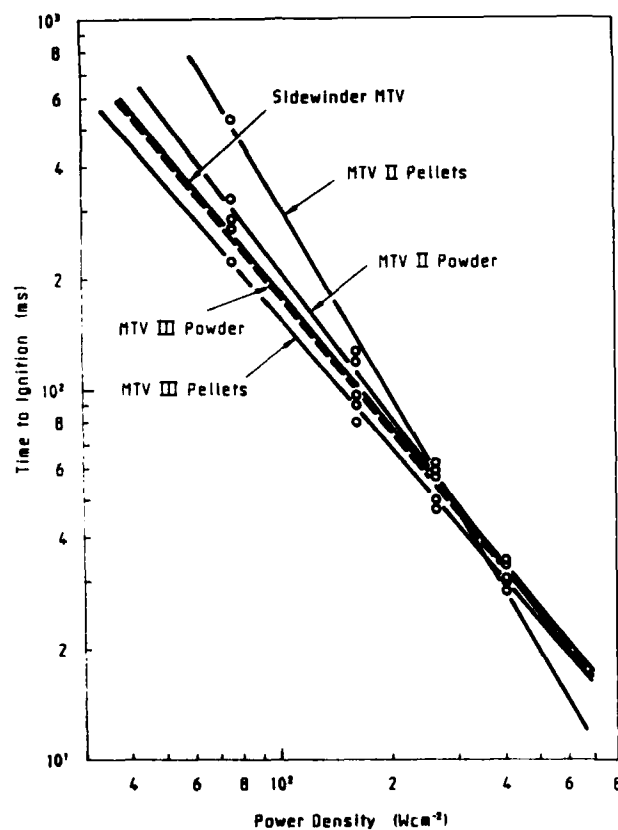
Figure 15　　*Relationship between Incident Laser Power Density and Time to Ignition for MTV Compositions (Powder, Pellets and Sidewinder Grain).*

37
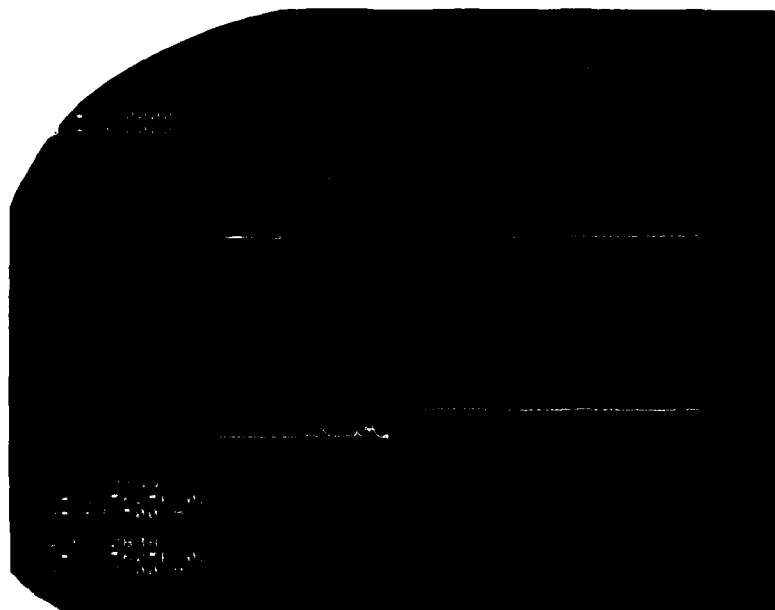
Figure 16   *Oscilloscope Response for Ignition of MTV Type III Powder at Incident Power De..sity of 160 W cm⁻².*
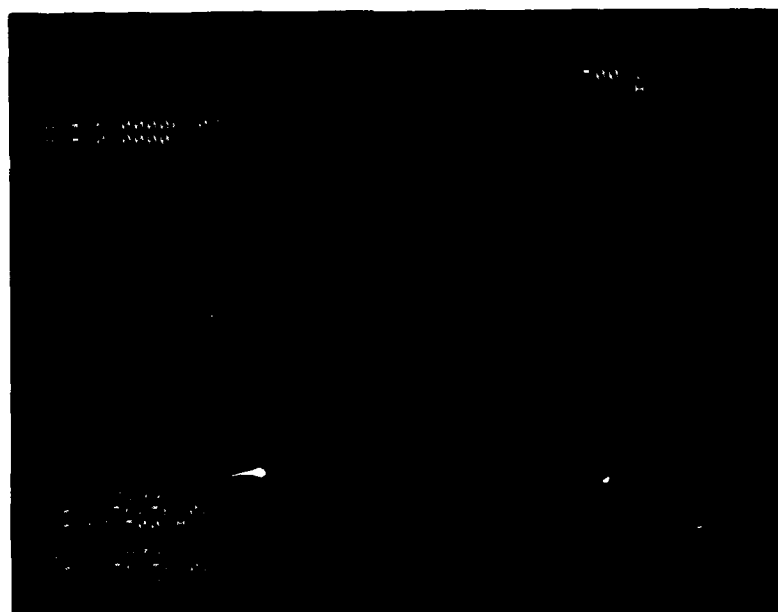
Figure 17   *Enlargement of Pre-Ignition Behaviour of MTV Type III Power (Figure 16) at Incident Power Density of 160 W cm⁻².*
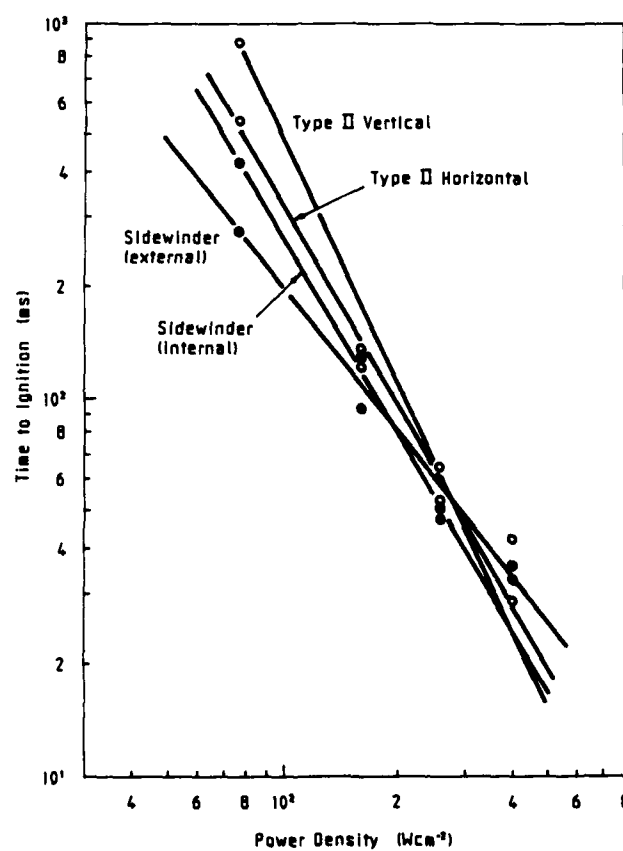
Figure 18 *Change in Time to Ignition with Incident Laser Power Density for Internal and External Sidewinder MTV and Vertical and Horizontal Type II MTV pellets.*
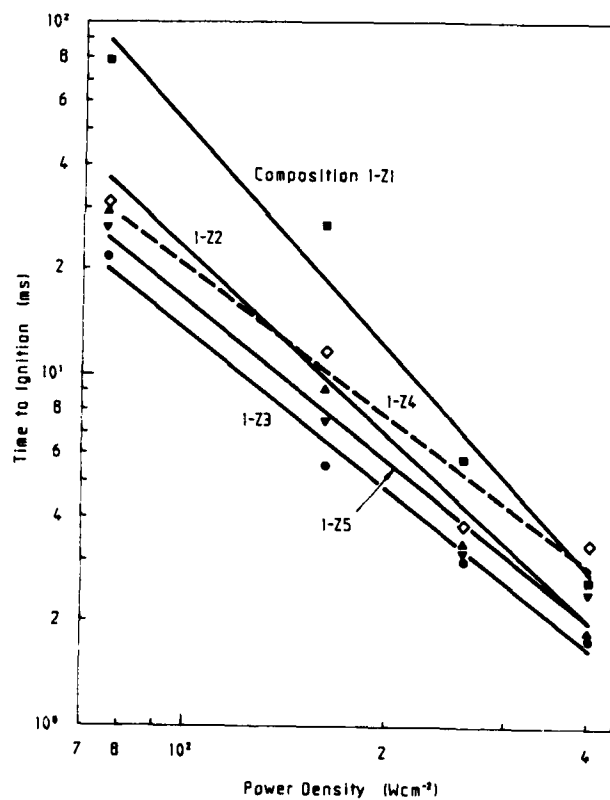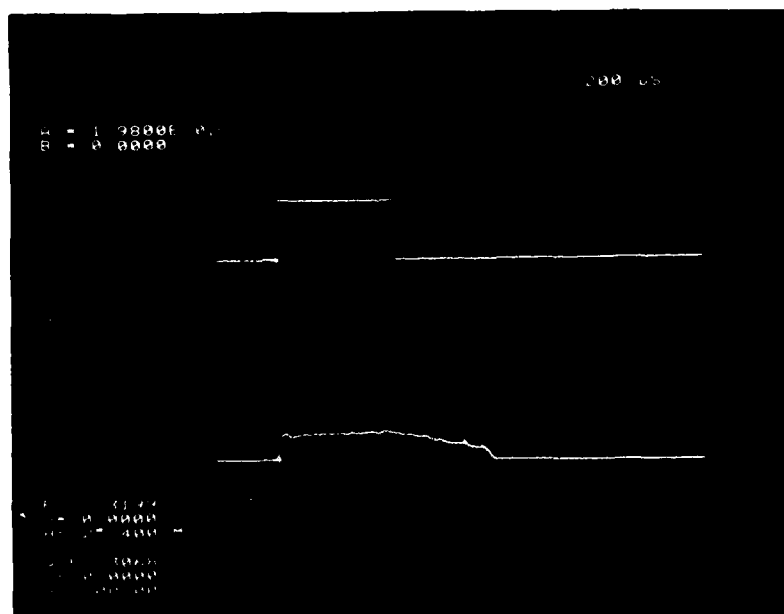
Figure 19   Relationship between Time to Ignition and Incident Laser Power
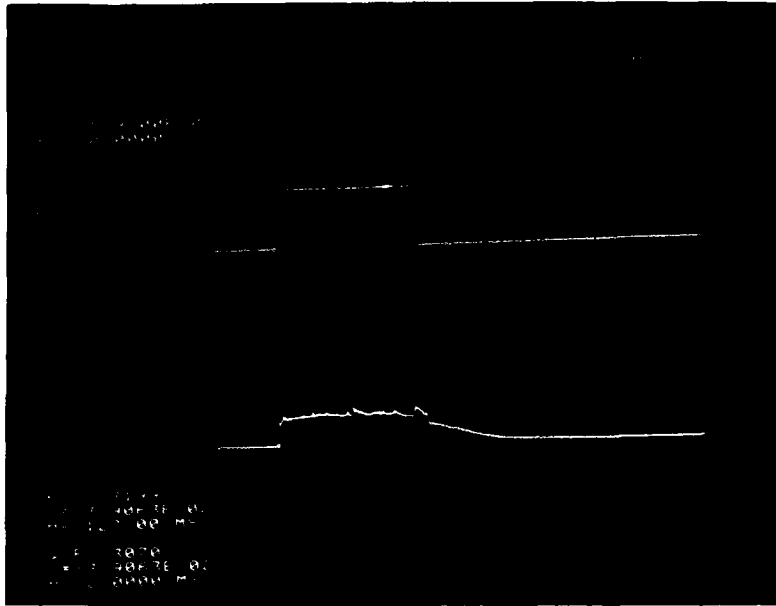Density for Zr/KClO₄/Graphite type Compositions (see Table 6).
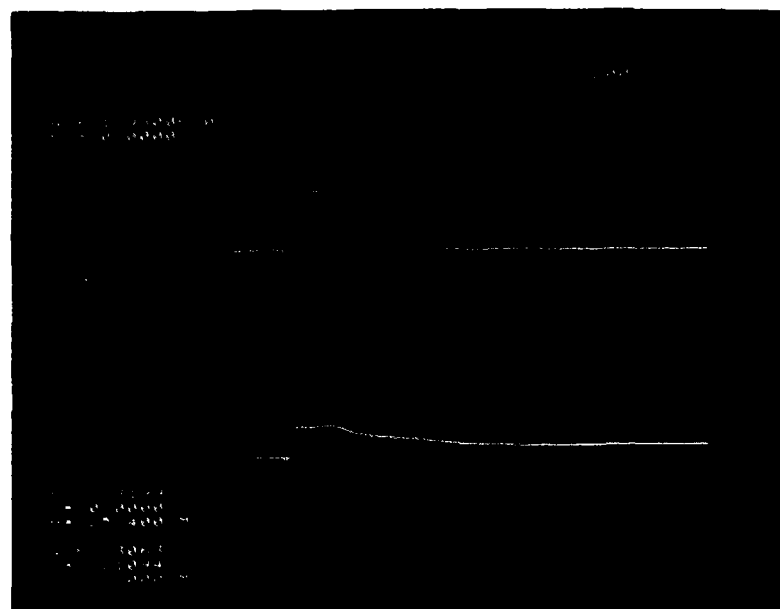
(a)

(b)

Figure 20   *Variation in Oscilloscope Response for Several Zr/KClO$_4$/Graphite Compositions at 400 W cm^{-2}.*
(a) 1-Z3   (b) 1-Z2   (c) 1-Z1

(c)
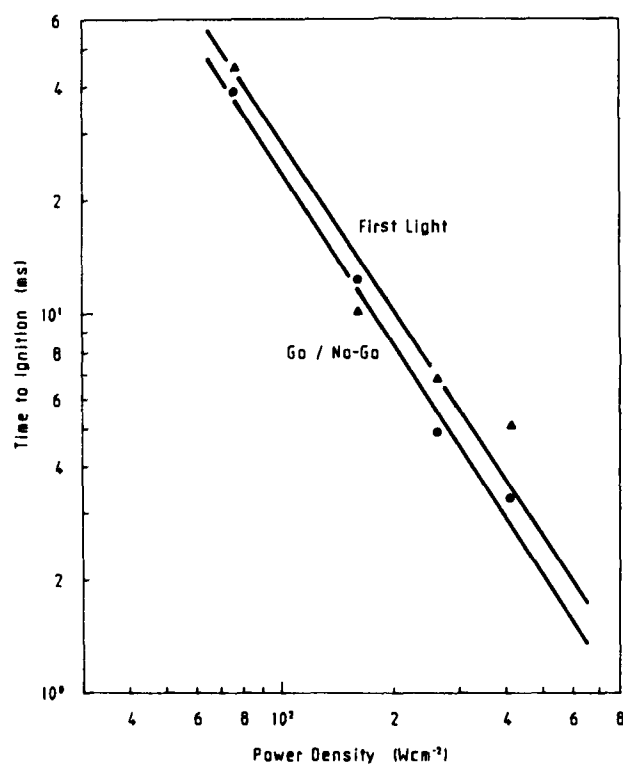
Figure 20 (continued)

Figure 21   *Effect of Different Ignition Criteria (First Light Versus Bruceton Go/No-Go) on the Time to Ignition for T-10 Delay Composition; ▲ First Light, ● Go/No-Go.*
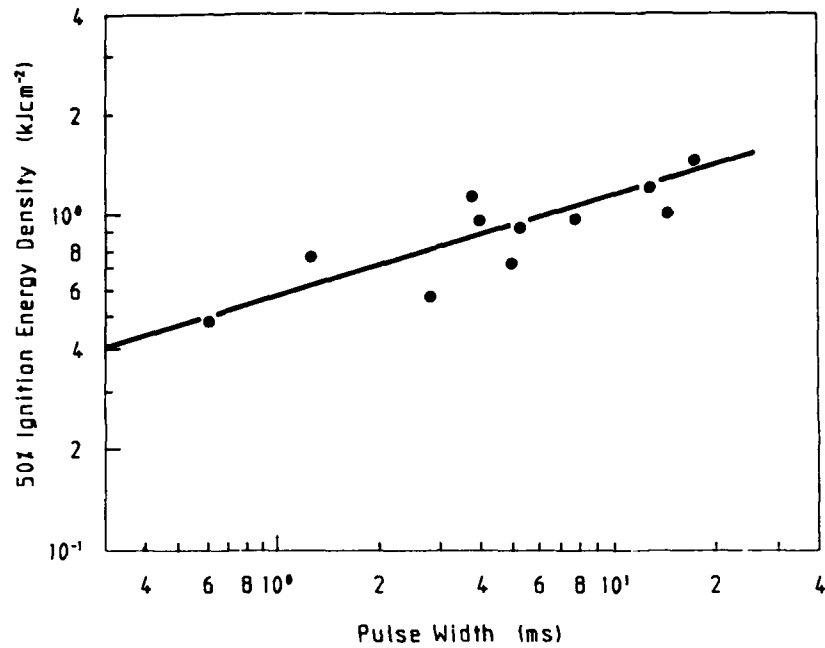
Figure 22   *Change in the Go/No-Go 50% Ignition Energy with Incident Laser Beam Pulse Length.*
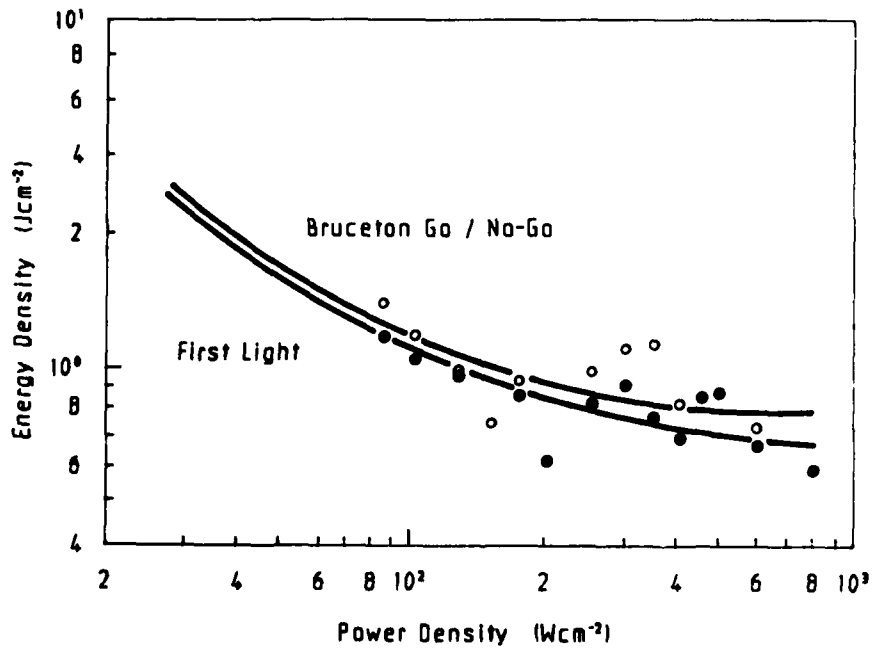

Figure 23   *Effect of Different Ignition Criteria on the Relationship between Ignition Energy Density and Power Density for A1A Composition;* • *First Light,* o *Go/No-Go.*
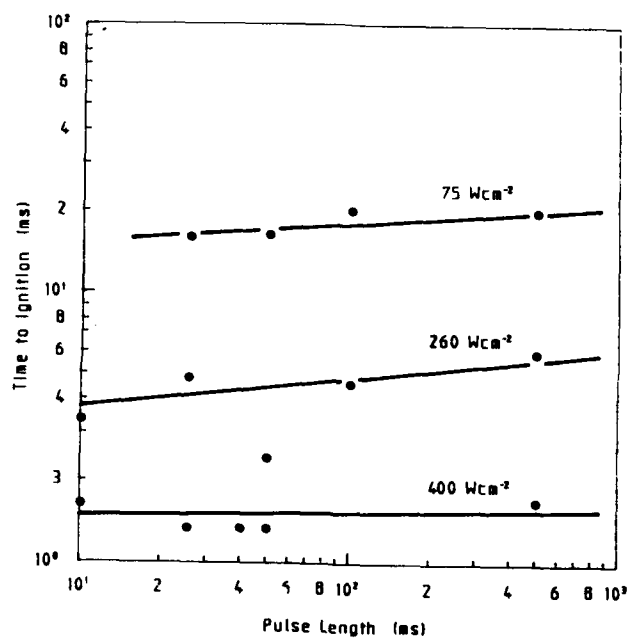
Figure 24   *Effect of Incident Laser Pulse Length on the Time to Ignition for A1A*
                  Composition at Several Power Densities.

45

DOCUMENT CONTROL DATA SHEET

REPORT NO. MRL-TR-90-*20*	AR NO. AR-006-*3/5*	REPORT SECURITY CLASSIFICATION Unclassified

TITLE

A study of the radiant ignition of a range of pyrotechnic
materials using a CO_2 laser

AUTHOR(S) L. de Yong, B. Park and F. Valenta	CORPORATE AUTHOR DSTO Materials Research Laboratory PO Box 50 Ascot Vale Victoria 3032

REPORT DATE August, 1990	TASK NO.	SPONSOR

FILE NO. G6/4/8-3852	REFERENCES 26	PAGES 46

CLASSIFICATION/LIMITATION REVIEW DATE	CLASSIFICATION/RELEASE AUTHORITY Chief, Explosives Division

SECONDARY DISTRIBUTION

Approved for public release

ANNOUNCEMENT

Announcement of this report is unlimited

KEYWORDS

Ignition	Pyrotechnics	Laser
Ignition Delay	Radiant Ignition	Power
Ignition Energy		

SUBJECT GROUPS

ABSTRACT

The ignition energy requirements for a range of pyrotechnic compositions of interest in both Australia and the United States have been measured experimentally using a 400 W CO_2 laser operating at 10.6 μm. The effects of several physical and chemical variables were determined on the time to ignition and ignition energy. The materials examined include a gasless delay, igniter compositions, a primer composition and a range of colored smoke compositions. The experimental data serves as a useful probe into ignition mechanisms, and may prove of value in the design of practical ignition systems.